Revision 2

Vasilseverginite, $Cu_9O_4(AsO_4)_2(SO_4)_2$, a new fumarolic mineral with a hybrid structure containing novel anion-centered tetrahedral structural units

Igor V. Pekov[1]*, Sergey N. Britvin[2,3], Sergey V. Krivovichev[3,2], Vasiliy O. Yapaskurt[1], Marina F. Vigasina[1], Anna G. Turchkova[1] and Evgeny G. Sidorov[4]

[1]Faculty of Geology, Moscow State University, Vorobievy Gory, 119991 Moscow, Russia

[2]Department of Crystallography, St Petersburg State University, Universitetskaya Nab. 7/9, 199034 St Petersburg, Russia

[3]Kola Science Center of Russian Academy of Sciences, Fersman Str. 18, 184209 Apatity, Russia

[4]Institute of Volcanology and Seismology, Far Eastern Branch of the Russian Academy of Sciences, Piip Boulevard 9, 683006 Petropavlovsk-Kamchatsky, Russia

*Corresponding author: igorpekov@mail.ru

This is the peer-reviewed, final accepted version for American Mineralogist, published by the Mineralogical Society of America.
The published version is subject to change. Cite as Authors (Year) Title. American Mineralogist, in press.
DOI: https://doi.org/10.2138/am-2020-7611. http://www.minsocam.org/

ABSTRACT

The new mineral vasilseverginite, ideally $Cu_9O_4(AsO_4)_2(SO_4)_2$, was found in the Arsenatnaya fumarole at the Second scoria cone of the Northern Breakthrough of the Great Tolbachik Fissure Eruption, Tolbachik volcano, Kamchatka, Russia. It is associated with tenorite, lammerite, stranskiite, lammerite-β, langbeinite, dolerophanite, sanidine, hematite, and gahnite. Vasilseverginite occurs as prismatic crystals up to 0.02×0.02×0.06 mm^3 combined in groups or interrupted crusts up to 1×2 cm^2 in area and up to 0.1 mm thick. It is transparent, bright green, with vitreous luster. D_{calc} is 4.41 $g·cm^{-3}$. Vasilseverginite is optically biaxial (–), α 1.816(5), β 1.870(5), γ 1.897(5), estimated $2V$ is 30(15)°. Chemical composition (wt.%, electron-microprobe) is: CuO 64.03, ZnO 0.79, Fe_2O_3 0.25, P_2O_5 0.05, As_2O_5 20.83, SO_3 14.92, total 100.87. The empirical formula calculated on O = 20 *apfu* is $(Cu_{8.78}Zn_{0.11}Fe^{3+}_{0.03})_{\Sigma 8.92}As_{1.98}P_{0.01}S_{2.03}O_{20}$. Vasilseverginite is monoclinic, $P2_1/n$, a = 8.1131(4), b = 9.9182(4), c = 11.0225(5) Å, β = 110.855(2)°, V = 828.84(6) $Å^3$, and Z = 2. The strongest reflections in the powder XRD pattern [d,Å(I)(hkl)] are: 7.13(41)(10-1), 5.99(70)(110, 11-1), 5.260(100)(101), 4.642(46)(111), 3.140(31)(03-1), 2.821(35)(02-3), 2.784(38)(13-2, 03-2), 2.597(35)(20-4), and 2.556(50)(23-1, 212). The crystal structure, solved using single-crystal X-ray diffraction data, R_1 = 0.025, is based upon complex $[O_4Cu_9]^{10+}$ layers parallel to (–101) that are composed of edge- and corner-sharing (OCu_4) tetrahedra. The topology is unprecedented in inorganic structural chemistry. The crystal structure can be considered a hybrid of the structures of popovite $Cu_5O_2(AsO_4)_2$ and dolerophanite $Cu_2O(SO_4)$ according to the scheme $Cu_9O_4(AsO_4)_2(SO_4)_2 = Cu_5O_2(AsO_4)_2 + 2Cu_2O(SO_4)$. The chemical hybridization does not result in a significant increase in chemical complexity of vasilseverginite compared to the sum of those of popovite and dolerophanite, whereas the structural hybridization leads to the doubling of structural information per unit cell. The mineral is named in memory of the outstanding Russian mineralogist, geologist and chemist Vasiliy Mikhailovich Severgin (1765–1826).

Keywords: vasilseverginite, new mineral, copper arsenate sulfate, popovite, dolerophanite, crystal structure, oxo-centered tetrahedra, structural complexity, hybridization of mineral species, fumarole sublimate, Tolbachik volcano

This is the peer-reviewed, final accepted version for American Mineralogist, published by the Mineralogical Society of America.
The published version is subject to change. Cite as Authors (Year) Title. American Mineralogist, in press.
DOI: https://doi.org/10.2138/am-2020-7611. http://www.minsocam.org/

INTRODUCTION

From the viewpoint of geochemical and environmental importance, sulfates and arsenates attract considerable attention as well, due to their existence in a wide range of geo- and cosmochemical environments. The ordered combination of arsenate and sulfate anions in the same mineral is rare; there are only twenty minerals known that contain both sulfate and arsenate as species-defining components. Among the twenty, only two species are H-free.

Natural H-bearing (with OH^- or/and H_2O) arsenate-sulfates usually have low-temperature, supergene origin and occur mainly in the oxidation zones of ore deposits. Among the members of the beudantite group, a subdivision of the alunite supergroup, only beudantite, $PbFe^{3+}_3(AsO_4)(SO_4)_2(OH)_6$, is a relatively common mineral, whereas other four species a rare, namely gallobeudantite, $PbGa_3(AsO_4)(SO_4)(OH)_6$, hidalgoite, $PbAl_3(AsO_4)(SO_4)_2(OH)_6$, kemmlitzite, $SrAl_3(AsO_4)(SO_4)_2(OH)_6$, and weilerite, $BaAl_3(AsO_4)(SO_4)_2(OH)_6$. In the crystal structures of some of these minerals, sulfate and arsenate anions are disordered, whereas others demonstrate ordered distribution of S^{6+} and As^{5+} over tetrahedral sites (Bayliss et al. 2010). The known hydrous Fe arsenate-sulfates are bukovskýite, $Fe^{3+}_2(AsO_4)(SO_4)(OH)\cdot 9H_2O$ (Majzlan et al. 2012), sarmientite, $Fe^{3+}_2(AsO_4)(SO_4)(OH)\cdot 5H_2O$ (Colombo et al. 2014), hilarionite, $Fe^{3+}_2(AsO_4)(SO_4)(OH)\cdot 6H_2O$ (Pekov et al. 2014), and zýkaite, $Fe^{3+}_4(AsO_4)_3(SO_4)(OH)\cdot 15H_2O$ (Čech et al. 1978). Bukovskýite and sarmientite are As,S-ordered minerals, whereas the crystal structures of hilarionite and zýkaite are unknown. For mallestigite, $Pb_3Sb(SO_4)(AsO_4)(OH)_6\cdot 3H_2O$ (Sima, 1998), the disordered distribution of As and S is likely, by analogy with other fleischerite-group members. In the crystal structure of juansilvaite, $Na_5Al_3[AsO_3(OH)]_4[AsO_2(OH)_2]_2(SO_4)_2\cdot 4H_2O$, sulfate groups and acid arsenate groups of two types demonstrate ordering (Kampf et al. 2017). Seven H-bearing arsenate-sulfates contain species-

73 defining Cu^{2+}. Arsentsumebite, $Pb_2Cu(AsO_4)(SO_4)(OH)$, a member of the brackebuschite group, has
74 partially ordered distribution of As and S (Zubkova et al. 2002), as well as sulfate-bearing variety of
75 thometzekite, a tsumcorite-group mineral with the idealized formula $PbCu_2(AsO_4)_2 \cdot 2H_2O$ (Krause et
76 al. 1998). As-S ordering was reported for chalcophyllite, $Cu_{18}Al_2(AsO_4)_4(SO_4)_3(OH)_{24} \cdot 36H_2O$
77 (Sabelli 1980), tangdanite, $Ca_2Cu_9(AsO_4)_4(SO_4)_{0.5}(OH)_9 \cdot 9H_2O$ (Ma et al. 2014), claraite,
78 $(Cu,Zn)_{15}(CO_3)_4(AsO_4)_2(SO_4)(OH)_{14} \cdot 7H_2O$ (Biagioni et al. 2017), and leogangite,
79 $Cu_{10}(AsO_4)_4(SO_4)(OH)_6 \cdot 8H_2O$ (Lengauer et al. 2004), and suggested for parnauite
80 $Cu_9(AsO_4)_2(SO_4)(OH)_{10} \cdot 7H_2O$ (Mills et al. 2013). The crystal structure of barrotite,
81 $Cu_9Al(HSiO_4)_2[(SO_4)(HAsO_4)_{0.5}](OH)_{12} \cdot 8H_2O$ (Sarp et al. 2014), is still unknown.

82 The H-free arsenates-sulfates are much rarer and are represented by nishanbaevite, ideally
83 $KAl_2O(AsO_4)(SO_4)$ (Pekov et al. 2019), and vasilseverginite, $Cu_9O_4(AsO_4)_2(SO_4)_2$, the mineral
84 described herein. Both minerals demonstrate an ordered distribution of AsO_4 and SO_4 tetrahedral
85 groups and contain additional oxygen atoms O_{ad}, not bonded to As^{5+} or S^{6+}. Both minerals are
86 unique to the active, oxidizing-type Arsenatnaya fumarole at the Tolbachik volcano (Kamchatka,
87 Russia), in which they were formed as volcanic sublimates under temperatures higher than 350–
88 400°C, like other arsenates described from this locality (Pekov et al. 2018a,b).

89 The new mineral vasilseverginite (Cyrillic: василсевергинит) is named in memory of the
90 outstanding Russian mineralogist, geologist and chemist Vasiliy Mikhailovich Severgin (1765–
91 1826), Academician of the Russian Academy of Sciences. He wrote the first books on geology and
92 mineralogy in Russia (Severgin 1791, 1798, 1807), created the first chemical nomenclature in
93 Russian and compiled the first Russian chemical dictionary. Acad. Severgin was one of the founders
94 of the Russian Mineralogical Society in 1817.

95 Both the new mineral and its name have been approved by the Commission on New
96 Minerals, Nomenclature and Classification of the International Mineralogical Association (IMA No.

2015–083). The type specimen is deposited in the systematic collection of the Fersman Mineralogical Museum of the Russian Academy of Sciences, Moscow under the catalogue number 95280.

ANALYTICAL METHODS

The chemical data for vasilseverginite were obtained using a Jeol JSM-6480LV scanning electron microscope equipped with an INCA-Wave 500 wavelength-dispersive spectrometer, with an acceleration voltage of 20 kV, a beam current of 20 nA, and a 3 μm beam diameter. The reference materials used are given in Table 1. Contents of other elements with atomic numbers higher than that of carbon are below detection limits.

The Raman spectrum of vasilseverginite was recorded using an EnSpectr R532 spectrometer with a green laser (532 nm) at room temperature. The laser beam output power was about 7 mW. The spectrum was processed using the EnSpectr expert mode program in the range from 100 to 4000 cm^{-1} with the use of a holographic diffraction grating with 1800 lines cm^{-1} and a resolution equal to 6 cm^{-1}. The diameter of the focal spot on the sample was about 10 μm. The Raman spectrum was acquired on a polycrystalline sample.

Powder X-ray diffraction (XRD) study of the new mineral was carried out using a Rigaku RAXIS Rapid II single-crystal diffractometer equipped with a curved image plate detector (Debye-Scherrer geometry, r = 127.4 mm) and Co$K\alpha$ radiation source (rotating anode, 40 kV, 15 mA), with Rigaku VariMax microfocus mirror optics. Imaging plate-to-profile data conversion was performed using osc2xrd software (Britvin et al. 2017).

A single-crystal X-ray dataset was collected by means of a Bruker Kappa APEX DUO diffractometer equipped with a microfocus Mo$K\alpha$ radiation source. A full Ewald sphere of reciprocal space was collected at a frame sweep of 1° to $2\Theta = 56°$. Data collection and refinement of unit-cell parameters were carried out using Bruker APEX2 software (Bruker 2003). Data processing

and integration routines were performed by means of a Rigaku Oxford Diffraction CrysAlisPro software. The crystal structure was solved by the intrinsic phasing method implemented in a *SHELXT*-2018 program (Sheldrick 2015) and refined to $R_1 = 0.025$ on the basis of 1428 unique observed [$I > 2\sigma(I)$] reflections, using *SHELXT*-2015 software incorporated into Olex2 graphical user interface (Dolomanov et al. 2009). A complete set of crystallographic data can be retrieved from the CIF file attached as the Supplementary Material.

The chemical and structural complexity parameters have been calculated using the procedure outlined by Krivovichev et al. (2018a,b). The chemical complexity was evaluated by the amounts of chemical Shannon information per atom (${}^{chem}I_G$) and per formula unit, f.u. (${}^{chem}I_{G,total}$), whereas the structural complexity was measured as the amounts of structural Shannon information per atom (${}^{str}I_G$) and per unit cell (${}^{str}I_{G,total}$).

RESULTS AND DISCUSSION

Occurrence and mineral association

The Arsenatnaya fumarole is situated at the apical part of the Second scoria cone of the Northern Breakthrough of the Great Tolbachik Fissure Eruption of 1975–1976. This scoria cone, a monogenetic volcano about 300 m high and approximately 0.1 km^3 in volume formed in 1975 (Fedotov and Markhinin 1983), is located 18 km South of the Ploskiy Tolbachik volcano in the central part of Kamchatka Peninsula, Far-Eastern Region, Russia (55°41'N 160°14'E, 1200 m asl). The fumarolic activity at this scoria cone remains strong: in 2012–2018, we observed here numerous gas vents with temperatures up to 490°C.

The specimens containing vasilseverginite were collected in July 2013 from the intermediate zone of the Arsenatnaya fumarole (Pekov et al. 2018a) located at a depth of 1–1.5 m from the day surface. The temperatures, measured during sampling by means of a chromel-alumel thermocouple in the pockets from which these specimens originate, were 360–380°C. We believe that

147 vsailseverginite was deposited directly from the gaseous phase as a volcanic sublimate at
148 temperatures higher than 380ºC.

149 On the holotype specimen, vasilseverginite occurs in intimate association with tenorite,
150 lammerite, lammerite-β, stranskiite, langbeinite, dolerophanite, hematite, As-bearing sanidine, and
151 Cu-bearing gahnite. On other specimens, the new mineral is associated also with johillerite,
152 urusovite, ericlaxmanite, kozyrevskite, popovite, tilasite, svabite, bradaczekite, aphthitalite,
153 metathénardite, belomarinaite, krasheninnikovite, anhydrite, euchlorine, wulffite,
154 alumoklyuchevskite, cryptochalcite, fluoborite, sylvite, and halite. The associated minerals are listed
155 in order of the decrease of abundance.

156

157 **General appearance, physical properties and optical data**

158 Vasilseverginite occurs as well-formed prismatic crystals up to 0.02×0.02×0.06 mm^3, with
159 complex oblique terminations (Fig. 1). The crystal forms were not determined. Vasilseverginite
160 crystals are combined in groups or interrupted, typically open-work incrustations (Figs. 1 and 2) up
161 to 1×2 cm^2 in area and up to 0.1 mm thick, usually overgrowing basalt scoria (Fig. 2a) or crystalline
162 crusts of tenorite (Fig. 2b).

163 Vasilseverginite is transparent, bright green, in some cases with a distinct golden hue. The
164 streak is light green. The lustre is vitreous. The mineral is brittle, cleavage or parting was not
165 observed, the fracture is uneven. The density and Mohs hardness were not measured because
166 crystals of vasilseverginite are too small and aggregates are open-work. The density calculated using
167 the empirical formula is 4.409 g cm^{-3}.

168 Under the microscope, in plane polarized transmitted light vasilseverginite is weakly
169 pleochroic: X = yellowish-green, Y and Z = emerald green. It is optically biaxial (–), α = 1.816(5), β
170 = 1.870(5), γ = 1.897(5) (589 nm), the estimated $2V$ value is 30(15)° and $2V_{calc.}$ = 69°. Such
171 difference between measured and calculated $2V$ values is probably caused by the low quality of

crystals, which is also reflected in the relatively high estimated errors ±0.005 for all three refractive indices. Dispersion of optical axes is weak, $r > v$.

Chemical composition

The chemical composition of the holotype specimen of vasilseverginite (in wt%, mean results for five spot analyses) are given in Table 1. The empirical formula calculated on the basis of 20 O atoms per formula unit is $(Cu_{8.78}Zn_{0.11}Fe^{3+}_{0.03})_{\Sigma 8.92}As_{1.98}P_{0.01}S_{2.03}O_{20}$. The idealized formula is $Cu_9O_4(AsO_4)_2(SO_4)_2$ which requires CuO 64.74, As_2O_5 20.78, SO_3 14.48, total 100 wt%.

Raman spectroscopy

The Raman spectrum of vasilseverginite is shown in Fig. 3. The Raman mode assignments, in accordance with Nakamoto (1986), are as follows. Bands with maxima at 1204, 1103 and 1075 cm^{-1} correspond to antisymmetric S^{6+}–O stretching vibrations, whereas those at 1007 and 982 cm^{-1} correspond to symmetric stretching vibrations of $(SO_4)^{2-}$ groups. The strongest single band at 846 cm^{-1} corresponds to As^{5+}–O stretching vibrations of $(AsO_4)^{3-}$ groups. The bands in the region 650–570 cm^{-1} correspond to S^{6+}–O bending vibrations. The strong band at 558 cm^{-1} could be assigned to Cu^{2+}–O stretching mode corresponding to short Cu–O distances, about 1.9–2.0 Å (Table 2). Bands with frequencies lower than 400 cm^{-1} probably correspond to As^{5+}–O bending vibrations, Cu^{2+}–O stretching vibrations corresponding to long Cu–O distances, about 2.3–2.4 Å (Table 2), and lattice modes. The absence of bands with Raman shifts higher than 1250 cm^{-1} indicates the absence of H-, C- and N-bearing groups in vasilseverginite.

Powder X-ray diffraction

Powder XRD data of vasilseverginite are reported in Table 3. The powder XRD pattern of the new mineral is unique and can be used as a good diagnostic tool. Parameters of the monoclinic

197 unit cell calculated from powder data are: a = 8.113(4), b = 9.918(2), c = 10.992(6) Å, β =
198 110.90(4)° and V = 826.2(8) Å^3.
199
200 **Crystal structure**
201 The crystal structure of vasilseverginite demonstrates a new structure type that has no
202 analogues among minerals and synthetic inorganic materials. It contains five symmetrically
203 independent Cu sites coordinated either by five (Cu1, Cu2, Cu4) or six (Cu3, Cu5) O atoms. The
204 Cu^{2+} coordination polyhedra are strongly distorted due to the Jahn-Teller effect (Fig. 4). The
205 description of the crystal structure of vasilseverginite in terms of cation coordination polyhedra is
206 very difficult because of the very complex system of linkage involving the distorted Cu square
207 pyramids and octahedra (Fig. 5a). In contrast, the description in terms of anion-centered (OCu_4)
208 tetrahedra (Krivovichev et al. 2013) formed by additional O_{ad} atoms (not bonded to As or S) is very
209 straightforward (Figs. 5b and 6). The O9 and O10 atoms are not bonded to As or S and are
210 coordinated tetrahedrally by four Cu atoms each, thus forming (OCu_4) oxocentered tetrahedra. The
211 structure is based upon complex $[O_4Cu_9]^{10+}$ layers composed of edge- and corner-sharing (OCu_4)
212 tetrahedra (Figs. 6c, d). The layers are parallel to (–101). The (SO_4) tetrahedra are located inside the
213 layers, whereas the (AsO_4) tetrahedra provide their linkage in the third dimension (Fig. 6a). It is
214 worthy to note that the topology of the $[O_4Cu_9]^{10+}$ layers is novel and unprecedented among known
215 minerals and synthetic compounds.
216
217 **Hybrid character of the structure and chemical and structural complexity**
218 In terms of chemistry, vasilseverginite has the composition intermediate between popovite,
219 $Cu_5O_2(AsO_4)_2$ (Pekov et al. 2015), and dolerophanite, $Cu_2O(SO_4)$ (Scacchi 1873; Effenberger
220 1985):
221 $$Cu_9O_4(AsO_4)_2(SO_4)_2 = Cu_5O_2(AsO_4)_2 + 2Cu_2O(SO_4) \quad (1)$$

Both dolerophanite and popovite have been found in the Tolbachik fumaroles and both contain structural units composed from edge- and corner-sharing (OCu_4) tetrahedra (Pekov et al. 2018b). However, the topologies and dimensionalities of the units are different. In dolerophanite, the (OCu_4) tetrahedra form sheets (Fig. 7a), whereas the crystal structure of popovite contains chains of alternating corner- and edge-linkage of (OCu_4) tetrahedra (Fig. 7b). In the dolerophanite sheet, all Cu atoms are bridging between adjacent (OCu_4) tetrahedra, either by sharing edges (the $Cu_{br[e]}$ atoms) or corners (the $Cu_{br[c]}$ atoms). In contrast, the $[O_2Cu_5]$ chain in popovite, along with the $Cu_{br[e]}$ and $Cu_{br[c]}$ atoms, contains also terminal Cu_t atoms that do not participate in the formation of the oxocentered structural unit. The $Cu_{br[e]}$:$Cu_{br[c]}$:Cu_t ratios in dolerophanite and popovite are equal to 1:1:0 and 2:1:2, respectively. The same ratio for vasilseverginite is equal to 4:3:2, which can easily be obtained as a sum of 2:2:0 (double dolerophanite ratio) and 2:1:2 (popovite ratio). Indeed, the topologies of the oxo-centered structural units in dolerophanite, popovite and vasilseverginite can be considered as based upon the same fundamental building block (FBB) consisting of four (OCu_4) tetrahedra sharing edges and corners (Figs. 6c, 7). These blocks are polymerized into infinite chains in popovite and into sheets in dolerophanite. The polymerization of the FBBs in vasilseverginite represents an intermediate case with the presence of terminal Cu_t atoms, but the resulting topology is two-dimensional.

Therefore, the crystal structure of vasilseverginite can be considered as a hybrid of the crystal structures of dolerophanite and popovite. The structural and chemical complexity parameters for the three minerals estimated using information-based measures (Krivovichev 2012, 2013, 2014; Krivovichev et al. 2018a,b) are given in Table 4. In both chemical and structural terms, the sequence of minerals in the order of decreasing complexity is vasilseverginite > popovite > dolerophanite. It is of interest that the chemical complexity of vasilseverginite (Vs) approximately corresponds to the sum of those of popovite (Po) and dolerophanite (Do), i.e. is described by the equation (1) (Vs = Po + 2Do):

This is the peer-reviewed, final accepted version for American Mineralogist, published by the Mineralogical Society of America.
The published version is subject to change. Cite as Authors (Year) Title. American Mineralogist, in press.
DOI: https://doi.org/10.2138/am-2020-7611. http://www.minsocam.org/

$$^{chem}I_{G,total}(Vs) = 47.498 \approx {}^{chem}I_{G,total}(Po) + 2\times{}^{chem}I_{G,total}(Do) = 42.867,$$

where $^{chem}I_{G,total}$ is the total amount of chemical Shannon information measured in bit per formula unit.

In contrast, the total structural complexity of Vs is approximately doubled compared to the sum of complexities of Po and Do:

$$^{str}I_{G,total}(Vs) = 268.930 \approx 2\times [{}^{str}I_{G,total}(Po) + 2\times{}^{str}I_{G,total}(Do)] = 282.974,$$

where $^{str}I_{G,total}$ is the total amount of structural Shannon information measured in bit per reduced unit cell.

Thus, the chemical hybridization of popovite and dolerophanite does not result in a significant increase in chemical complexity (the sum of their chemical information amounts is approximately equal to that of vasilseverginite), whereas the structural hybridization leads to the doubling of structural information per unit cell (the structural information of vasilseverginite is doubled compared to the sum of structural information amounts of popovite and dolerophanite).

IMPLICATIONS

It has recently been mentioned that one of the aspects that a new mineral discovery may provide is an insight into crystal chemistry or the structures of natural and synthetic phases (Barton 2019). The discovery of vasilseverginite brings a new insight into the modularity of structures with anion-centered tetrahedral units based upon (OCu_4) tetrahedra. Vasilseverginite is both a chemical and a structural hybrid of popovite and dolerophanite, and the hybridization results in the formation of a new structure type with a novel layer topology. The Cu compounds with oxo-centered clusters, either polymerized or forming polyoxocuprate clusters (Kondinski and Monakhov 2017), attract much attention in condensed matter physics and materials chemistry, due to their interesting

magnetic properties (Volkova and Marinin 2018; Botana et al. 2018; Badrtdinov et al. 2018; Winiarski et al. 2019), and new mineralogical discoveries may provide important insights into pathways of the preparation of novel synthetic compounds (Britvin et al. 2020; Siidra et al. 2020). The concept of hybridization of mineral species developed in this work may bring new ideas for the preparation of novel structural architectures on the border of stability fields of chemically and structurally simpler compounds.

The discovery of vasilseverginite also provides further indirect evidence for the existence of polynuclear oxo-centered copper clusters in the gaseous phase (Kovrugin et al. 2015), which may serve as a means of transport for Cu by volcanic gases in fumaroles, thus enhancing the mobility of metals in volcanic environments.

ACKNOWLEDGMENTS

We thank referees Anthony R. Kampf and Gerald Giester and Associate Editor Charles Geiger for valuable comments. This work was supported by the Russian Science Foundation, grants nos. 19-17-00050 (mineralogical characterization, chemical and spectroscopic studies) and 19-17-00038 (crystal chemical study and complexity analysis). The SEM and EMPA studies were performed in the Laboratory of Analytical Techniques of High Spatial Resolution, Dept. of Petrology, Moscow State University. The technical support by the St. Petersburg State University X-Ray Diffraction Resource Center is acknowledged.

REFERENCES CITED

294 Badrtdinov, D.I., Kuznetsova, E.S., Verchenko, V.Yu., Berdonosov, P.S., Dolgikh, V.A.,
295 Mazurenko, V.V., and Tsirlin, A.A. (2018) Magnetism of coupled spin tetrahedra in ilinskite-
296 type $KCu_5O_2(SeO_3)_2Cl_3$. Scientific Reports 8, 2379.
297 Barton, I.F. (2019) Trends in the discovery of new minerals over the last century. American
298 Mineralogist, 104, 641-651.
299 Bayliss, P., Kolitsch, U., Nickel, E.H., and Pring, A. (2010) Alunite supergroup: recommended
300 nomenclature. Mineralogical Magazine, 74, 919-927.
301 Biagioni, C. and Orlandi, P. (2017) Claraite, $(Cu,Zn)_{15}(AsO_4)_2(CO_3)_4(SO_4)(OH)_{14}\cdot 7H_2O$:
302 redefinition and crystal structure. European Journal of Mineralogy, 29, 1031-1044.
303 Botana, A.S., Zheng, H., Lapidus, S.H., Mitchell, J.F., and Norman, M.R. (2018) Averievite: A
304 copper oxide kagome antiferromagnet. Physical Review, B98, 054421.
305 Britvin, S.N., Dolivo-Dobrovolsky, D.V., and Krzhizhanovskaya, M.G. (2017) Software for
306 processing the X-ray powder diffraction data obtained from the curved image plate detector of
307 Rigaku RAXIS Rapid II diffractometer. Zapiski Rossiiskogo Mineralogicheskogo
308 Obshchestva, 146(3), 104–107 (in Russian).
309 Britvin, S.N., Pekov, I.V., Yapaskurt, V.O., Koshlyakova, N.N., Göttlicher, J., Krivovichev, S.V.,
310 Turchkova, A.V., and Sidorov, E.G. (2020) Polyoxometalate chemistry at volcanoes:
311 discovery of a novel class of polyoxocuprate nanoclusters in fumarolic minerals. Scientific
312 Reports, 10, 6345.
313 Bruker (2003) SAINT (ver. 7.60A). Bruker AXS Inc., Madison, Wisconsin, USA.
314 Čech, F., Praha, J., and Novak, F. (1978) Zýkaite, $Fe^{3+}_4(AsO_4)_3(SO_4)(OH)\cdot 15H_2O$, a new mineral.
315 Neues Jahrbuch für Mineralogie, Monatshefte, 134-144.
316 Colombo, F., Rius, J., Vallcorba, O., and Miner, E.P. (2014) The crystal structure of sarmientite,
317 $Fe^{3+}_2(AsO_4)(SO_4)(OH)\cdot 5H_2O$, solved ab initio from laboratory powder diffraction data.
318 Mineralogical Magazine, 78, 347-360.

319 Dolomanov, O.V., Bourhis, L.J., Gildea, R.J., Howard, J.A., and Puschmann, H. (2009) OLEX2: a
320 complete structure solution, refinement and analysis program. Journal of Applied
321 Crystallography, 42, 339-341.
322 Effenberger, H. (1985) $Cu_2O(SO_4)$, dolerophanite: refinement of the crystal structure with a
323 comparison of $OCu(II)_4$ tetrahedra in inorganic compounds. Monatschefte für Chemie, 116,
324 927-931.
325 Fedotov, S.A. and Markhinin, Y.K., eds. (1983) The Great Tolbachik Fissure Eruption. Cambridge
326 University Press, NY.
327 Kampf, A.R., Nash, B.P., Dini, M., and Molina Donoso, A.A. (2017) Juansilvaite,
328 $Na_5Al_3[AsO_3(OH)]_4[AsO_2(OH)_2]_2(SO_4)_2 \cdot 4H_2O$, a new arsenate-sulfate from the Torrecillas
329 mine, Iquique Province, Chile. Mineralogical Magazine, 81, 619-628.
330 Kondinski, A. and Monakhov, K.Y. (2017) Breaking the Gordian knot in the structural chemistry of
331 polyoxometalates: copper(II)-oxo/hydroxo clusters. Chemistry - a European Journal, 23, 7841-
332 7852.
333 Kovrugin, V.M., Siidra, O.I., Colmont, M., Mentre, O., and Krivovichev, S.V. (2015) Emulating
334 exhalative chemistry: synthesis and structural characterization of ilinskite,
335 $Na[Cu_5O_2](SeO_3)_2Cl_3$, and its K-analogue. Mineralogy and Petrology, 109, 421-430.
336 Krause, W., Belendorff, K., Bernhardt, H.-J., McCammon C., Effenberger, H., and Mikenda, W.
337 (1998) Crystal chemistry of the tsumcorite-group minerals. New data on ferrilotharmeyerite,
338 tsumcorite, thometzekite, mounanaite, helmutwinklerite, and a redefinition of gartrellite.
339 European Journal of Mineralogy, 10, 179-206.
340 Krivovichev, S.V. (2012) Topological complexity of crystal structures: quantitative approach. Acta
341 Crystallographica, A68, 393-398.
342 Krivovichev, S.V. (2013) Structural complexity of minerals: information storage and processing in
343 the mineral world. Mineralogical Magazine, 77, 275-326.

344 Krivovichev, S.V. (2014) Which inorganic structures are the most complex? Angewandte Chemie
345 International Edition, 53, 654-661.
346 Krivovichev, S.V., Mentre, O., Siidra, O.I., Colmont, M., and Filatov, S.K. (2013) Anion-centered
347 tetrahedra in inorganic compounds. Chemical Reviews, 113, 6459-6535.
348 Krivovichev, V.G., Charykova, M.V., and Krivovichev, S.V. (2018a) The concept of mineral
349 systems and its application to the study of mineral diversity and evolution. European Journal
350 of Mineralogy, 30, 219-230.
351 Krivovichev, S.V., Krivovichev, V.G., and Hazen, R.M. (2018b) Structural and chemical
352 complexity of minerals: correlations and time evolution. European Journal of Mineralogy, 30,
353 231-236.
354 Lengauer, C.L., Giester, G., and Kirchner, E. (2004) Leogangite, $Cu_{10}(AsO_4)_4(SO_4)(OH)_6 \cdot 8H_2O$, a
355 new mineral from the Leogang mining district, Salzburg province, Austria. Mineralogy and
356 Petrology, 81, 187-201.
357 Ma, Z., Li, G., Chukanov, N.V., Poirier, G., and Shi, N. (2014) Tangdanite, a new mineral species
358 from the Yunnan Province, China and the discreditation of 'clinotyrolite'. Mineralogical
359 Magazine, 78, 559-569.
360 Majzlan, J., Lazic, B., Armbruster, T., Johnson, M.B., White, M.A., Fisher, R.A., Plášil, J., Loun, J.,
361 Škoda, R., and Novák, M. (2012) Crystal structure, thermodynamic properties, and paragenesis
362 of bukovskýite, $Fe_2(AsO_4)(SO_4)(OH) \cdot 9H_2O$. Journal of Mineralogical and Petrological
363 Sciences, 107, 133-148.
364 Mills, S.J., Kampf, A.R., McDonald, A.M., Bindi, L., Christy, A.G., Kolitsch, U., and Favreau, G.
365 (2013) The crystal structure of parnauite: a copper arsenate–sulphate with translational
366 disorder of structural rods. European Journal of Mineralogy, 25, 693-704.
367 Nakamoto, K. (1986) Infrared and Raman Spectra of Inorganic and Coordination Compounds. John
368 Wiley & Sons, NY.

Pekov, I.V., Chukanov, N.V., Yapaskurt, V.O., Rusakov, V.S., Belakovskiy, D.I., Turchkova, A.G., Voudouris, P., Magganas, A., and Katerinopoulos, A. (2014) Hilarionite, $Fe^{3+}_2(SO_4)(AsO_4)(OH)\cdot 6H_2O$, a new supergene mineral from Lavrion, Greece. Geology of Ore Deposits, 56(7) (Special Issue: Zapiski of the Russian Mineralogical Society), 567-575.

Pekov, I.V., Zubkova, N.V., Yapaskurt, V.O., Belakovskiy, D.I., Vigasina, M.F., Sidorov, E.G., and Pushcharovsky, D.Y. (2015). New arsenate minerals from the Arsenatnaya fumarole, Tolbachik volcano, Kamchatka, Russia. III. Popovite, $Cu_5O_2(AsO_4)_2$. Mineralogical Magazine, 79, 133-143.

Pekov, I.V., Koshlyakova, N.N., Zubkova, N.V., Lykova, I.S., Britvin, S.N., Yapaskurt, V.O., Agakhanov, A.A., Shchipalkina, N.V., Turchkova, A.G., and Sidorov, E.G. (2018a) Fumarolic arsenates – a special type of arsenic mineralization. European Journal of Mineralogy, 30, 305-322.

Pekov, I.V., Zubkova, N.V., and Pushcharovsky, D.Yu. (2018b) Copper minerals from volcanic exhalations – a unique family of natural compounds: crystal chemical review. Acta Crystallographica, B74, 502-518.

Pekov, I.V., Zubkova, N.V., Yapaskurt, V.O., Belakovskiy, D.I., Britvin, S.N., Agakhanov, A.A., Turchkova, A.G., Sidorov, E.G., and Pushcharovsky D.Y. (2019) Nishanbaevite, IMA 2019-012. CNMNC Newsletter No. 50, October 2019, page 616. Mineralogical Magazine, 31, 615-620.

Sabelli, C. (1980) The crystal structure of chalcophyllite. Zeitschrift für Kristallographie, 151, 129-140.

Sarp H., Černy R., Puscharovsky D.Yu., Schouwink P., Teyssier J., Williams P.A., Babalik H., Mari G. (2014) La barrotite, $Cu_9Al(HSiO_4)_2[(SO_4)(HAsO_4)_{0.5}](OH)_{12}\cdot 8H_2O$, un nouveau minéral de la mine de Roua (Alpes-Maritimes, France). Riviera Scientifique, 98, 3-22.

Scacchi, A. (1873) Nuove specie di solfati di rame (Dolerofano). Note Mineralogiche, Memoria Prima, Napoli, Stamperia del Fibreno, pp. 22-29.

Severgin, V. (1791) Elementary Foundations of Natural History, 2 vols. Imperial Typography, St. Petersburg (in Russian).

Severgin, V. (1798) Elementary Foundations of Mineralogy, or Natural History of Minerals, 2 vols. Imperial Typography, St. Petersburg (in Russian).

Severgin, V. (1807) Detailed Mineralogical Dictionary, 2 vols. Imperial Academy of Sciences Publishing, St. Petersburg (in Russian).

Sheldrick, G.M. (2015) Crystal structure refinement with *SHELXL*. Acta Crystallographica, C71, 3-8.

Siidra, O.I., Vladimirova, V.A., Tsirlin, A.A., Chukanov, N.V., and Ugolkov, V.L. (2020) $Cu_9O_2(VO_4)_4Cl_2$, the first copper oxychloride vanadate: mineralogically inspired synthesis and magnetic behavior. Inorganic Chemistry, 59, 2136–2143.

Sima, I. (1998) Mallestigit, $Pb_3Sb(SO_4)(AsO_4)(OH)_6{\cdot}3H_2O$, ein neues Mineral von einer Halde des ehemaligen Cu-Pb-Zn-Bergbaues NW des Mallestiger Mittagskogels in den Westkarawanken, Kärnten, Österreich. Mitteilungen der Österreichischen Mineralogischen Gesellschaft, 143, 225-227.

Volkova, L.M. and Marinin, D.V. (2018) Antiferromagnetic spin-frustrated layers of corner-sharing Cu_4 tetrahedra on the kagome lattice in volcanic minerals $Cu_5O_2(VO_4)_2(CuCl)$, $NaCu_5O_2(SeO_3)_2Cl_3$, and $K_2Cu_5Cl_8(OH)_4{\bullet}2H_2O$. Journal of Physics, Condensed Matter, 30, 425801.

Winiarski, M.J., Tran, T.T., Chamorro, J.R., and McQueen, T.M. (2019) $(CsX)Cu_5O_2(PO_4)_2$ (X = Cl, Br, I): a family of Cu^{2+} $S = 1/2$ Compounds with capped-Kagomé networks composed of OCu_4 units. Inorganic Chemistry, 58, 4328–4336.

417 Zubkova, N.V., Pushcharovsky, D.Yu., Giester, G., Tillmanns, E., Pekov, I.V., and Kleimenov D.A.

418 (2002) The crystal structure of arsentsumebite, $Pb_2Cu[(As,S)O_4]_2(OH)$. Mineralogy and

419 Petrology, 75, 79-88.

420 **Figure captions**

421

422 **Figure 1.** Typical crystal group (a) and crystal crust (b) of vasilseverginite. SEM (SE) images.

423

424 **Figure 2.** Bright green aggregares of vasilseverginite on basalt scoria with iron-black tenorite and
425 white sanidine (a) and on iron-black tenorite crystal crust with light blue stranskiite (b). Photo: I.V.
426 Pekov and A.V. Kasatkin.

427

428 **Figure 3.** The Raman spectrum of vasilseverginite (only region with Raman bands is shown).

429

430 **Figure 4.** Coordination polyhedra of Cu^{2+} cations in the crystal structure of vasilseverginite.
431 Legend: Cu atoms = green; O atoms = red. Displacement ellipsoids are drawn at 75% probability
432 level. Cu–O bonds longer than 2.078 Å are shown as thin grey lines.

433

434 **Figure 5.** Crystal structure of vasilseverginite shown with cation-centered coordination polyhedra
435 (a) and as a combination of $(SO_4)^{2-}$ and $(AsO_4)^{3-}$ tetrahedra and $[O_4Cu_9]^{10+}$ double layers consisting
436 of edge- and corner-sharing (OCu_4) tetrahedra (b).

437

438 **Figure 6.** The $[O_4Cu_9]^{10+}$ double layer in the crystal structure of vasilseverginite surrounded by
439 $(SO_4)^{2-}$ and $(AsO_4)^{3-}$ tetrahedra (a) and the same layer shown as ball-and-stick (b) and polyhedral (c)
440 representations. The dotted line in (c) outlines the contour of the tetramer of edge- and corner-
441 sharing tetrahedra.

442

443 **Figure 7**. The $[O_2Cu_4]^{4+}$ sheet in dolerophanite (a) and the arrangement of the $[O_2Cu_5]^{6+}$ chains in
444 popovite (b). The dotted lines outline the contours of the tetramers of edge- and corner-sharing
445 tetrahedra.
446
447

This is the peer-reviewed, final accepted version for American Mineralogist, published by the Mineralogical Society of America.
The published version is subject to change. Cite as Authors (Year) Title. American Mineralogist, in press.
DOI: https://doi.org/10.2138/am-2020-7611. http://www.minsocam.org/

448

449

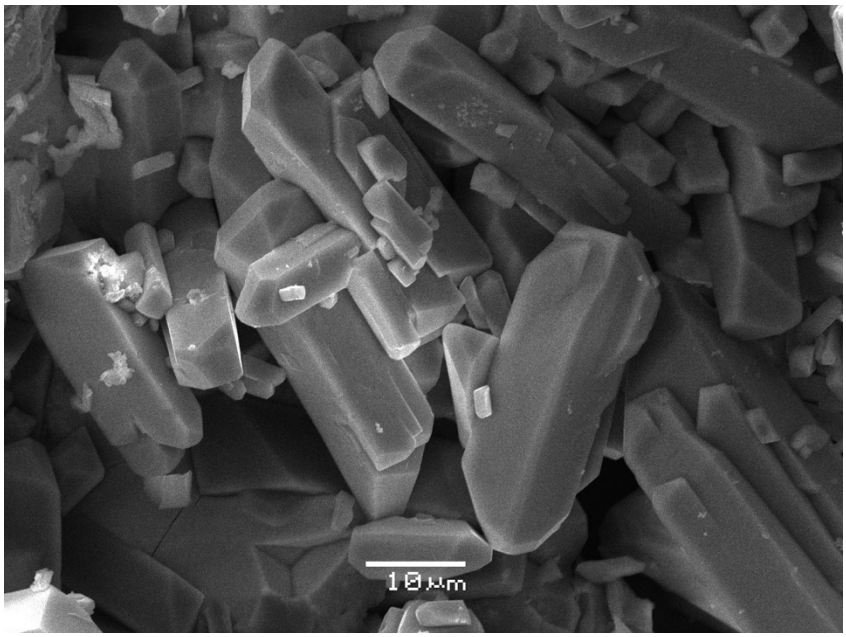

450
451
452 **Figure 1a**
453

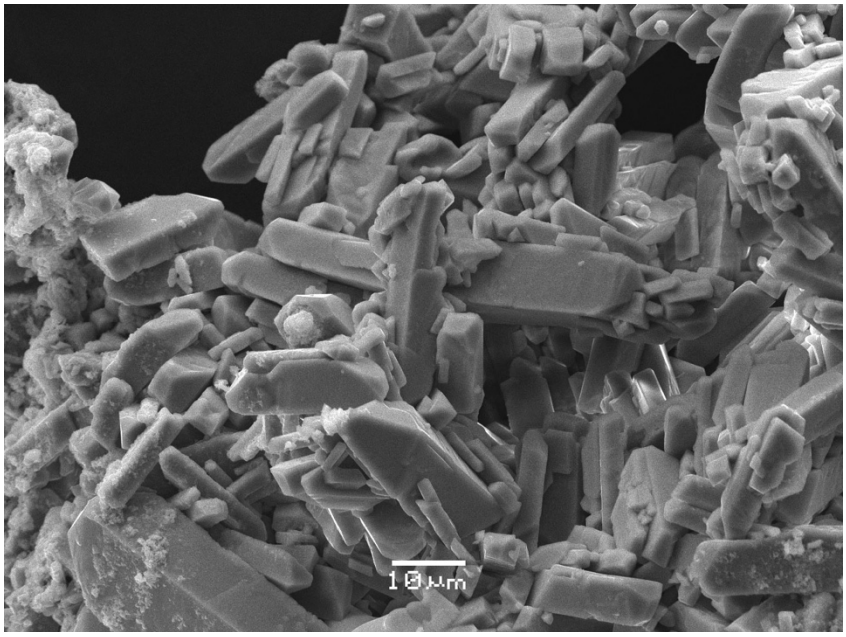

454
455
456 **Figure 1b**

This is the peer-reviewed, final accepted version for American Mineralogist, published by the Mineralogical Society of America.
The published version is subject to change. Cite as Authors (Year) Title. American Mineralogist, in press.
DOI: https://doi.org/10.2138/am-2020-7611. http://www.minsocam.org/

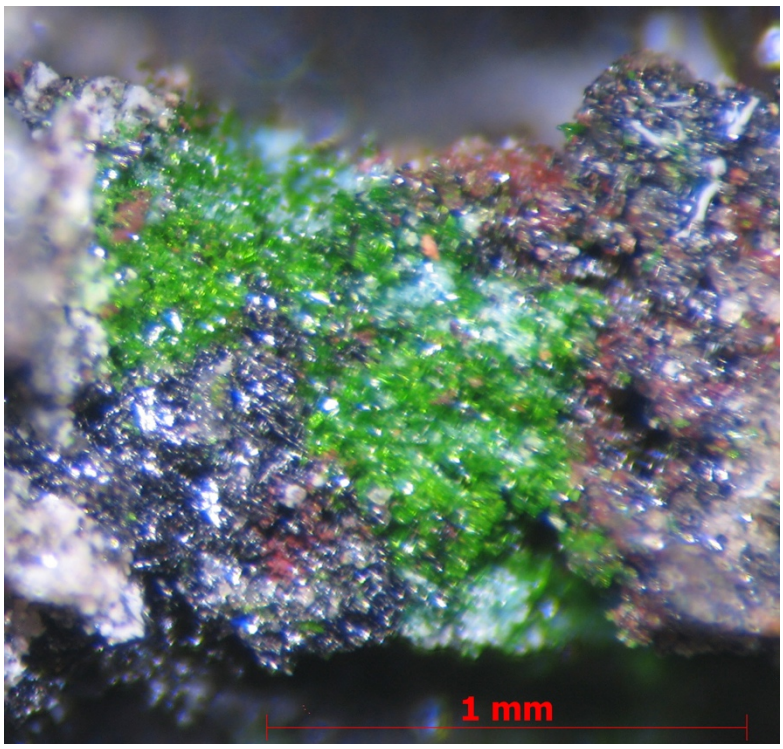

Figure 2a

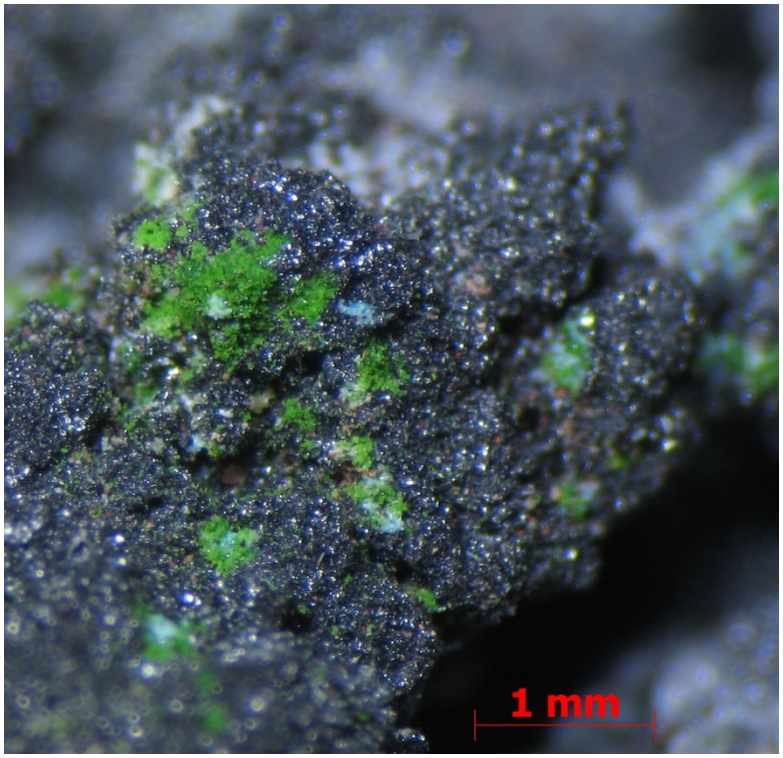

Figure 2b

This is the peer-reviewed, final accepted version for American Mineralogist, published by the Mineralogical Society of America.
The published version is subject to change. Cite as Authors (Year) Title. American Mineralogist, in press.
DOI: https://doi.org/10.2138/am-2020-7611. http://www.minsocam.org/

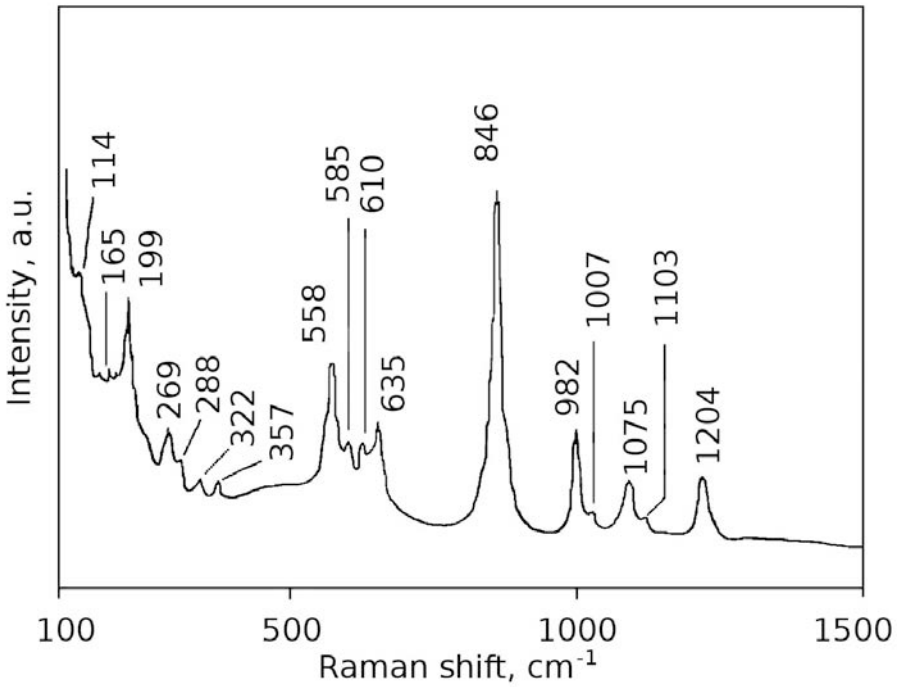

Figure 3

This is the peer-reviewed, final accepted version for American Mineralogist, published by the Mineralogical Society of America.
The published version is subject to change. Cite as Authors (Year) Title. American Mineralogist, in press.
DOI: https://doi.org/10.2138/am-2020-7611. http://www.minsocam.org/

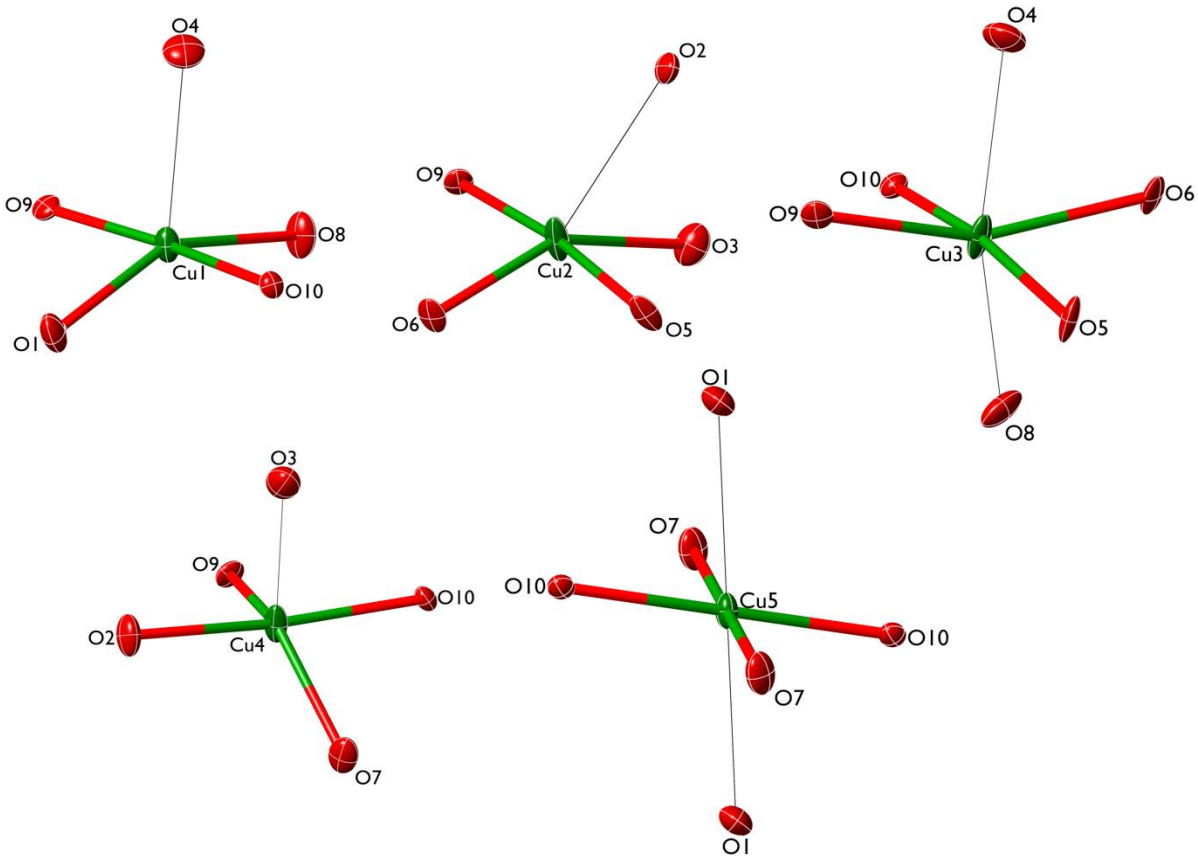

Figure 4

This is the peer-reviewed, final accepted version for American Mineralogist, published by the Mineralogical Society of America.
The published version is subject to change. Cite as Authors (Year) Title. American Mineralogist, in press.
DOI: https://doi.org/10.2138/am-2020-7611. http://www.minsocam.org/

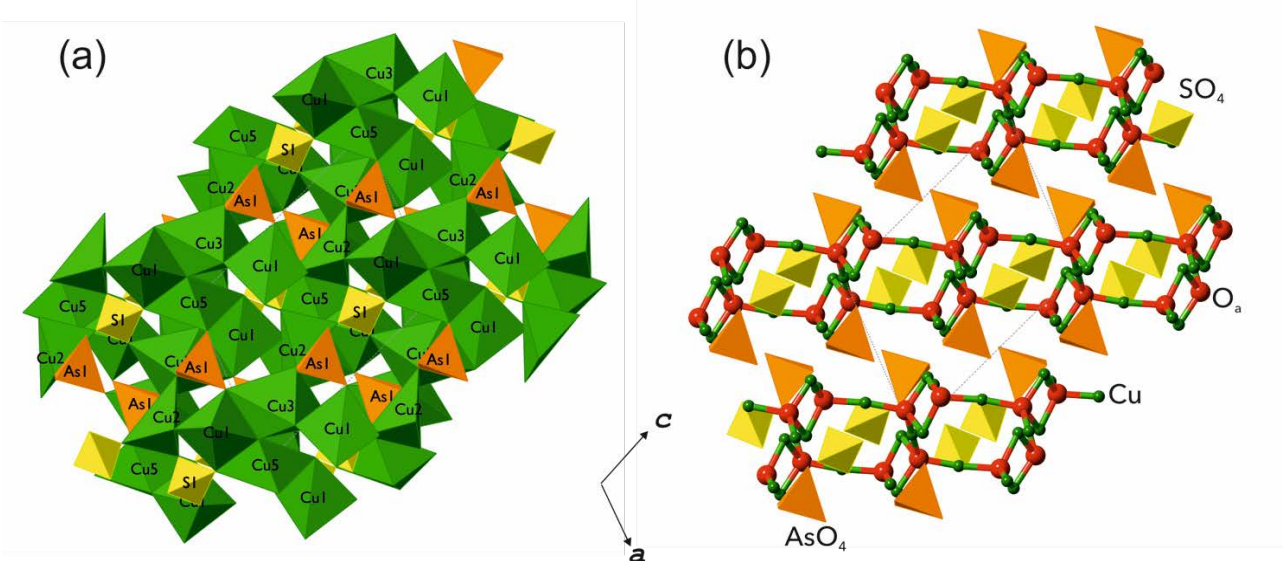

Figure 5

This is the peer-reviewed, final accepted version for American Mineralogist, published by the Mineralogical Society of America.
The published version is subject to change. Cite as Authors (Year) Title. American Mineralogist, in press.
DOI: https://doi.org/10.2138/am-2020-7611. http://www.minsocam.org/

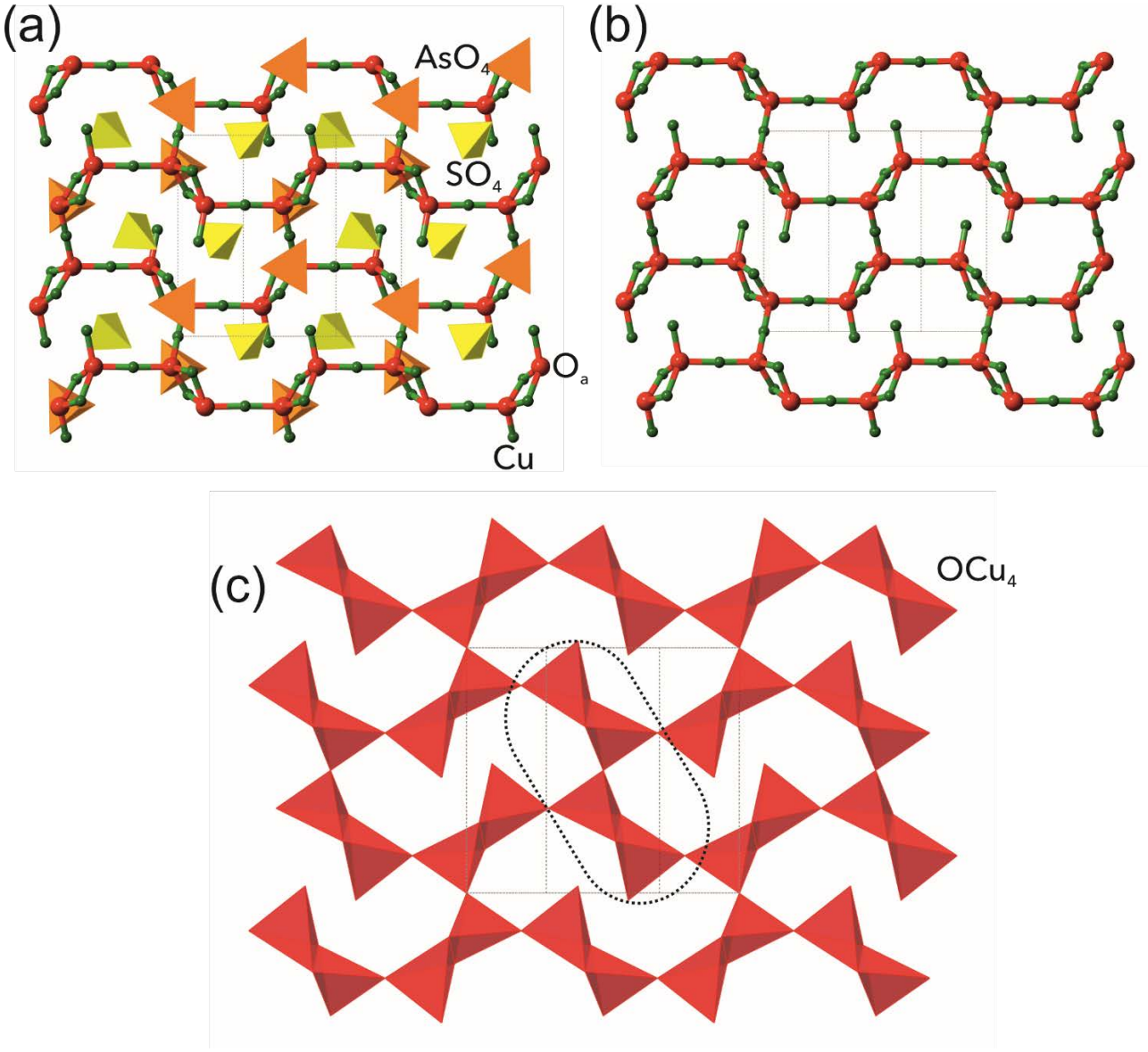

480
481
482 **Figure 6**
483

This is the peer-reviewed, final accepted version for American Mineralogist, published by the Mineralogical Society of America.
The published version is subject to change. Cite as Authors (Year) Title. American Mineralogist, in press.
DOI: https://doi.org/10.2138/am-2020-7611. http://www.minsocam.org/

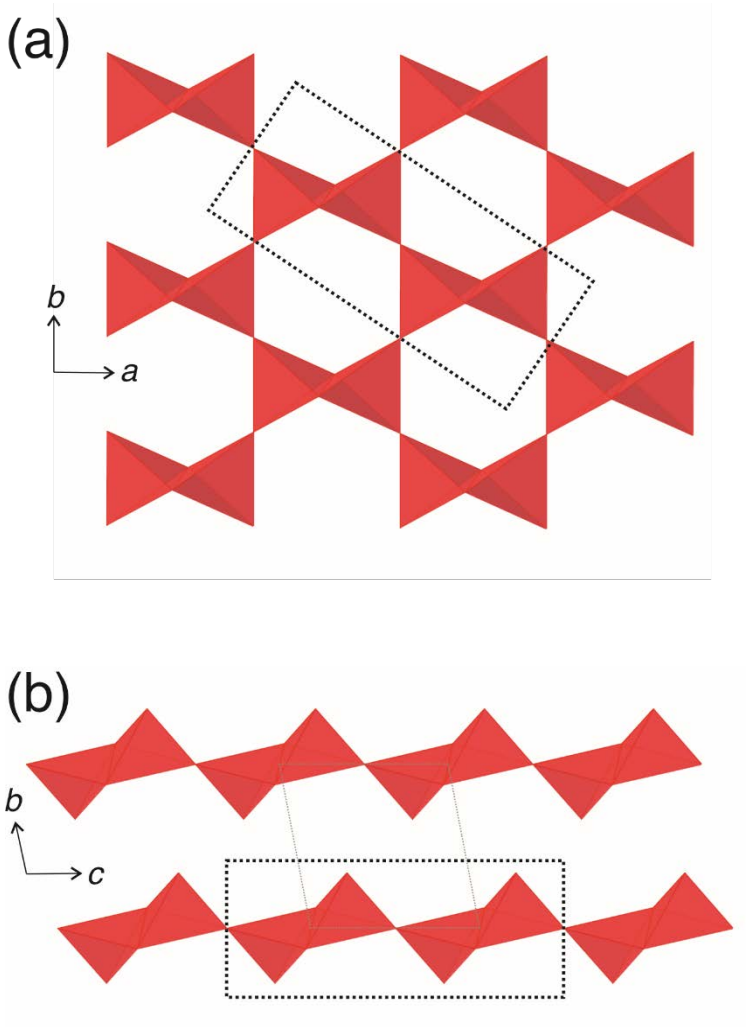

Figure 7

This is the peer-reviewed, final accepted version for American Mineralogist, published by the Mineralogical Society of America.
The published version is subject to change. Cite as Authors (Year) Title. American Mineralogist, in press.
DOI: https://doi.org/10.2138/am-2020-7611. http://www.minsocam.org/

488 **Tables**

489

490 **Table 1.** Chemical composition (wt%) of vasilseverginite

491

Constituent	Mean	Range	Standard Deviation	Reference Material
CuO	64.03	63.53–64.52	0.44	$CuFeS_2$
ZnO	0.79	0.09–1.30	0.61	ZnS
Fe_2O_3*	0.25	0.00–0.60	0.25	FeS
P_2O_5	0.05	0.00–0.14	0.05	GaP
As_2O_5	20.83	20.13–21.48	0.56	FeAsS
SO_3	14.92	13.14–15.83	1.03	$SrSO_4$
Total	100.87			

492

493 * Fe is considered as trivalent, owing to the extremely oxidizing conditions in the Arsenatnaya

494 fumarole (Pekov et al. 2018a).

495

496

497 **Table 2.** Selected bond lengths (Å) for vasilseverginite

Bond	**Distance**	**Bond**	**Distance**
Cu1−O1	2.039(3)	S−O1	1.490(3)
Cu1−O4	2.295(3)	S−O2	1.501(3)
Cu1−O8	1.986(3)	S−O3	1.504(3)
Cu1−O9	1.982(3)	S−O4	1.453(3)
Cu1−O10	1.941(3)	<S−O>	1.487
<Cu1−O>	2.049	As−O5	1.708(3)
Cu2−O3	2.071(3)	As−O6	1.702(3)
Cu2−O5	1.971(3)	As−O7	1.685(3)

Cu2−O6	1.975(3)	As−O8	1.668(3)
Cu2−O9	1.901(3)	<As−O>	1.691
Cu2−O4	2.440(3)		
<Cu2−O>	2.072	O9−Cu1	1.982(3)
Cu3−O5	1.936(3)	O9−Cu2	1.901(3)
Cu3−O6	2.027(3)	O9−Cu3	2.034(3)
Cu3−O9	2.034(3)	O9−Cu4	1.994(3)
Cu3−O10	1.886(3)	<O9−Cu>	1.978
Cu3−O4	2.530(3)		
Cu3−O8	2.641(3)		
<Cu3−O>	2.083	O10−Cu1	1.941(3)
Cu4−O2	1.965(3)	O10−Cu3	1.886(3)
Cu4−O3	2.390(3)	O10−Cu4	1.900(3)
Cu4−O7	2.035(3)	O10−Cu5	1.914(3)
Cu4−O9	1.994(3)	<O10−Cu>	1.910
Cu4−O10	1.900(3)		
<Cu4−O>	2.096		
Cu5−O1 × 2	2.390(3)		
Cu5−O7 × 2	2.031(3)		
Cu5−O10 × 2	1.914(3)		
<Cu5−O>	2.112		

500 **Table 3.** Powder X-ray diffraction data (d in Å) for vasilseverginite

I_{obs}	d_{obs}	I_{calc}*	d_{calc}**	$h\ k\ l$
19	7.50	13	7.515	10-1
41	**7.13**	40	7.144	01-1
70	**5.99**	31, 44	6.023, 5.990	110, 11-1
100	**5.260**	100	5.275	101
46	**4.642**	41	4.657	111
21	4.560	20	4.571	01-2
2	4.465	2	4.468	02-1
16	4.134	8, 6	4.150, 4.139	120, 12-1
18	3.780	19	3.791	200
5	3.651	3	3.655	10-3
14	3.565	14, 1	3.572, 3.541	02-2, 210
7	3.502	7	3.514	21-2
28	3.451	25	3.461	112
12	3.238	12	3.244	01-3
31	**3.140**	29, 4	3.148, 3.140	03-1, 22-1
11	3.049	4	3.051	211
15	3.021	13, 3, 2, 1	3.030, 3.026, 3.017, 3.012	130, 13-1, 21-3, 220
18	2.959	20	2.962	122
35	**2.821**	23	2.823	02-3
38	**2.784**	36, 25	2.791, 2.782	13-2, 03-2
27	2.668	41, 2, 1	2.675, 2.669, 2.655	113, 22-3, 11-4
18	2.630	30	2.637	202
35	**2.597**	68, 3	2.604, 2.592	20-4, 31-1
17	2.588	14	2.584	31-2
50	**2.556**	92, 11	2.563, 2.549	23-1, 212
3	2.498	11, 1	2.505, 2.493	30-3, 01-4
3	2.475	2, 1	2.482, 2.479	23-2, 040
6	2.438	5, 7	2.449, 2.429	310, 31-3
5	2.420	2	2.424	123

18	2.374	32, 14	2.381, 2.362	03-3, 32-1
15	2.353	12, 5	2.355, 3.355	32-2, 14-1
4	2.282	2	2.285	02-4
8	2.239	12, 1	2.244, 2.239	141, 14-2
4	2.207	6	2.217	311
9	2.188	10, 10	2.196, 2.192	10-5, 31-4
3	2.150	7, 5	2.157, 2.144	114, 11-5
5	2.132	8	2.135	213
2	2.108	1	2.112	21-5
9	2.067	8, 2	2.070, 2.067	24-2, 321
5	2.047	2, 1	2.052, 2.046	14-3, 23-4
7	2.022	7, 1, 1	2.028, 2.019, 2.017	40-2, 124, 01-5
6	2.003	6, 4, 2	2.010, 2.008, 2.001	04-3, 330, 223
3	1.973	5, 3	1.979, 1.964	30-5, 312
2	1.956	1, 1, 1	1.961, 1.956, 1.952	241, 41-1, 243
3	1.936	5	1.940	31-5
3	1.914	7	1.918	15-1
2	1.897	2	1.902	02-5
3	1.870	1, 4	1.874, 1.862	331, 410
12	1.853	19, 3, 1, 2, 1	1.858, 1.857, 1.851, 1.851, 1.850	322, 151, 05-2, 42-1, 143
3	1.832	1, 3	1.838, 1.830	32-5, 105
3	1.825	1, 2	1.824, 1.822	233, 34-1
5	1.804	4, 4	1.809, 1.806	23-5, 242
7	1.784	6	1.786	04-4
3	1.759	7, 2	1.762, 1.758	34-3, 250
5	1.713	1, 6	1.717, 1.717	125, 006
3	1.696	2, 6	1.698, 1.692	33-5, 01-6
4	1.671	2	1.676	341
5	1.651	10	1.653	060
2	1.628	3, 2, 1	1.632, 1.629, 1.622	06-1, 24-5, 02-6
2	1.610	2	1.612	234
3	1.593	3	1.595	51-3

6	1.569	8, 1	1.571, 1.570	05-4, 44-2
8	1.553	11, 4, 3, 1, 2	1.559, 1.555, 1.555, 1.554, 1.552	342, 35-3, 51-4, 21-7, 333
5	1.545	7	1.546	34-5
12	1.534	13, 14, 1, 6	1.537, 1.537, 1.536, 1.533	43-5, 33-6, 52-3, 11-7
7	1.494	11	1.495	351
4	1.486	5, 2	1.487, 1.487	126, 35-4
3	1.464	5	1.465	26-3
3	1.432	6, 1	1.434, 1.432	343, 235
7	1.417	7, 2, 6	1.421, 1.417, 1.414	23-7, 16-4, 511
5	1.410	3, 1	1.411, 1.408	02-7, 36-1
6	1.397	1, 3, 2, 1, 8	1.401, 1.401, 1.399, 1.396, 1.396	35-5, 262, 51-6, 423, 26-4
3	1.376	3, 1, 2	1.378, 1.378, 1.375	530, 20-8, 305
2	1.357	3, 3	1.359, 1.356	52-6, 54-2
2	1.353	2	1.354	54-3
3	1.341	4, 1, 1, 2, 1	1.345, 1.344, 1.344, 1.343, 1.339	155, 03-7, 25-6, 60-2, 11-8
2	1.323	4, 1, 2, 1	1.326, 1.324, 1.323, 1.321	61-4, 164, 172, 16-5
2	1.315	3, 1	1.316, 1.313	50-7, 26-5
1	1.297	2	1.298	05-6
1	1.294	3	1.293	27-3
2	1.287	3, 2	1.289, 1.285	06-5, 54-5

*For the calculated pattern, only reflections with intensities ≥1 are given; **for the unit-cell parameters calculated from single-crystal data. The strongest observed reflections are marked in bold type.

This is the peer-reviewed, final accepted version for American Mineralogist, published by the Mineralogical Society of America.
The published version is subject to change. Cite as Authors (Year) Title. American Mineralogist, in press.
DOI: https://doi.org/10.2138/am-2020-7611. http://www.minsocam.org/

Table 4. Information-based chemical and structural complexity parameters for dolerophanite, popovite and vasilseverginite [v in atoms per cell; I_G in bit per atom; $I_{G,total}$ in bit per formula (chem) or per cell (str)]

Mineral	Formula	Sp. gr.	Chemical complexity			Structural complexity		
			^{chem}v	$^{chem}I_G$	$^{chem}I_{G,total}$	^{str}v	$^{str}I_G$	$^{str}I_{G,total}$
Dolerophanite	$Cu_2O(SO_4)$	$C2/m$	8	1.299	10.392	16	2.750	44.000
Popovite	$Cu_5O_2(AsO_4)_2$	$P\text{-}1$	17	1.299	22.083	17	3.146	53.487
Vasilseverginite	$Cu_9O_4(AsO_4)_2(SO_4)_2$	$P2_1/n$	33	1.439	47.498	66	4.075	268.930